Near-Infrared Spectroscopy and Imaging for the Monitoring of Powder Blend Homogeneity

ARWA S. EL-HAGRASY,[1] HANNAH R. MORRIS,[2] FRANK D'AMICO,[3] ROBERT A. LODDER,[4] JAMES K. DRENNEN III[1]

[1]Graduate School of Pharmaceutical Sciences, Duquesne University, Pittsburgh, Pennsylvania 15282

[2]Carnegie Mellon Research Institute, Pittsburgh, Pennsylvania

[3]Department of Computational Mathematics, McAnulty College and Graduate School of Liberal Arts, Duquesne University, Pittsburgh, Pennsylvania

[4]College of Pharmacy, University of Kentucky, Lexington, Kentucky

Received 15 November 2000; revised 27 March 2001; accepted 28 March 2001

ABSTRACT: In-process testing requirements for adequacy of mixing are established in 21 CFR 211.110(a)(3). Considering also, the U.S. Food and Drug Administration's draft guidance published in 1999 (Guidance for Industry, ANDAs: Blend Uniformity Analysis; http://www.fda.gov/cder/guidance/index.htm), the importance of when and how to perform blend uniformity analysis is obvious. Near-infrared (NIR) spectroscopy was used noninvasively, in this study, to monitor powder blend homogeneity. Powder mixtures consisting of salicylic acid and Fast-Flo lactose were blended in an 8-qt. V-Blender. Optical ports installed at six positions on the blender allowed spectral collection using fiber optics. A traditional thief probe was used to collect powder samples for ultraviolet (UV) reference analysis. The blender was stopped at preselected time points for collection of NIR and UV data. Several algorithms and sampling protocols were studied to identify an optimum methodology for blend homogeneity determination. The blending process was also monitored with an InSb imaging camera for comparison with the traditional NIR spectroscopy and UV reference data. Data analysis indicates that multiple sampling points were essential for accurate and precise estimation of mixing end points. Moreover, multiple runs of identical blends often display homogeneity at unique end points, thus demonstrating the potential advantage of monitoring every blend.
J Pharm Sci 90:1298–1307, 2001

Keywords: NIR (near-infrared); blend uniformity analysis; homogeneity; process control; imaging

INTRODUCTION

In light of the ongoing discussion about the U.S. Food and Drug Administration's (FDA's) draft guidance on blend uniformity analysis (Guidance for Industry, ANDAs: Blend Uniformity Analysis; http://www.fda.gov/cder/guidance/index.htm) and the general lack of understanding of blending processes, new technology allowing improved control of such mixing processes should be of significant interest to a large audience. Blending of solids and semisolids is a critical step in the production of many pharmaceutical products. Homogeneity of blends is essential for obtaining high quality products of uniform content. The intent of any blending process is to achieve a uniform mixture of all ingredients including active and excipient(s). Lack of content uniformity can

Correspondence to: J. K. Drennen, III (Telephone: 412-396-6315; Fax: 412-396-4660; E-mail: drennen@duq.edu)

Journal of Pharmaceutical Sciences, Vol. 90, 1298–1307 (2001)

lead to product recall by the FDA for sub-potency or super-potency reasons. Recalls for sub-potency represent the second top reason for drug recalls in 1999 (http://www.fda.gov/cder/reports/ rtn00-3.htm).

Standard mixing practice in certain pharmaceutical settings involves processing in a blender for a predetermined period of time, after which samples are removed from the blender with a thief probe and then analyzed by high-performance liquid chromatography (HPLC) or ultraviolet (UV) spectroscopy to determine the concentration of active ingredient. If the analytical results indicate content uniformity, then the blended materials are released for further processing.

This conventional method of monitoring blend uniformity involves invasive sampling procedures. Significant sampling error is often associated with the use of thief probes for removal of samples from powder blenders. Such sampling devices disturb the powder bed and compromise the validity of collected samples. If particle size variations exist between the individual components, segregation can be a significant concern during powder flow into the sample compartment of the thief probe. Segregation prevents representative sampling of the blend. Another significant factor adding to the error associated with such invasive sampling is variability between operators during sample collection. Any change in the insertion angle or twisting of the probe can affect powder flow into the sample thief.[1–4]

Although research continues in an attempt to identify an ideal thief probe,[5] noninvasive sampling could ultimately provide the least sampling error.

An alternate method for blend monitoring is to remotely sample the blend using near-infrared (NIR) spectroscopy. NIR spectroscopy has found increasing use in pharmaceutical analysis for identification and quality testing of raw materials,[6,7] for analysis of intact tablets for a wide variety of properties,[8–10] for analysis of parenteral products,[11] for determination of ointment homogeneity and many other applications.[12] NIR monitoring is a noninvasive technique that minimizes analysis times and sample preparation while eliminating the sampling bias associated with the disruption and removal of samples from the blender by a sample thief. Because nearly all pharmaceutically important compounds exhibit some NIR spectrum, NIR methods provide a means of determining the homogeneity of all components in a blend. NIR spectroscopy has been used before to assess the homogeneity of powder blends from thieved powder samples.[13] The feasibility of single-point monitoring of powder blending in a V-blender by NIR spectroscopy has also been established.[14]

This study will examine the blending of a model two-component system consisting of salicylic acid and lactose. The importance of both the number and position of multiple sampling ports was investigated. NIR monitoring of powder blending at a single location on a blender versus multiple locations was evaluated. A detailed comparison of NIR spectroscopy, NIR imaging, and the UV reference method was performed. Spectral preprocessing techniques play a vital role in NIR identification of the end point of mixing and are discussed. Minor environmental (humidity, temperature, static charge, etc.) and physicochemical (active concentration, particle size, etc.) variations can have a significant impact on the end point of any mixing process and are discussed.

EXPERIMENTAL SECTION

Materials

Salicylic acid (SA; Fischer Scientific, Pittsburgh, PA) and Fast-Flo lactose (Foremost, Baraboo, WI) were used as received. Methanol (Fischer Scientific, Pittsburgh, PA) was OPTIMA grade.

Mixing

A plastic 8-qt. V-blender (Patterson-Kelly Company, Inc., East Stroudsburg, PA) was used for the mixing studies. The model powder blend was a two-component mixture consisting of 3, 7, or 11% SA as the active ingredient and lactose as the excipient. Powders were loaded into the blender from the left side. Lactose was loaded first, followed by SA. The blender was filled with powders to 90% (v/v) of working capacity, which is within the range of filling levels commonly used in the industry.[15]The blender was rotated at 23 rpm.

The blending process was monitored for 30 min and the blender was stopped at predetermined times to sample the powder. A thief probe (made in-house) was used to collect powder samples equivalent to ~1 g from six different locations in the powder bed, as shown in Figure 1. The active ingredient was extracted and analyzed by UV spectroscopy as described later.

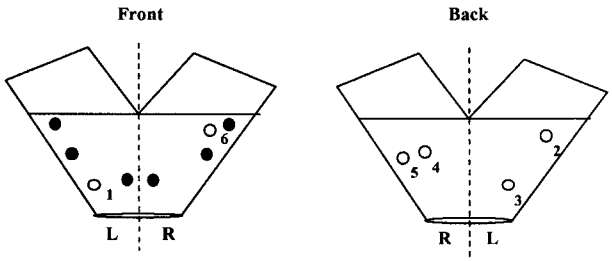

Figure 1. V-Blender showing NIR sampling ports (○) and UV sampling points (●).

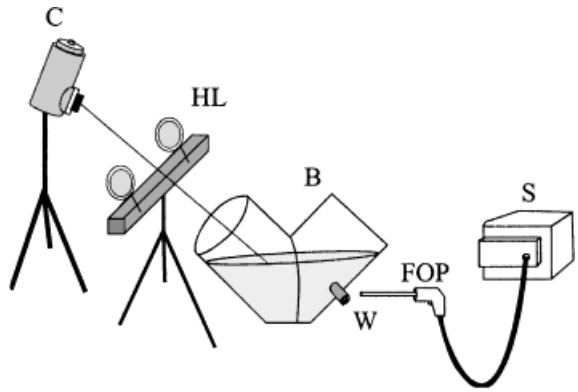

Figure 2. NIR imaging setup: InSb camera (C), heat lamps (HL), V-blender (B), sapphire window (W), spectrophotometer (S), and fiber-optic probe (FOP).

Near-Infrared Spectroscopy

Six sapphire windows (Edmund Scientific Company, Barrington, NJ) were mounted at different locations on the V-blender. NIR spectra were collected with an NIRSystems Model 5000 monochromator (Foss NIRSystems, Silver Spring, MD) equipped with a fiber-optic probe (420 fibers, 2.55-m fiber bundle). The fiber-optic probe was used to monitor the blending process remotely and noninvasively. Locations of the optical ports are shown in Figure 1. Blending was halted at the specified time points, and the probe was positioned against each of the windows to collect spectra. Spectra were analyzed over the range1100–2200 nm. A visual inspection of the optical ports insured that the powder did not stick to the windows.

Collected spectra were transformed using various preprocessing algorithms to study the effect of each in determining the end point of mixing. Preprocessing treatments [second derivative, standard normal variate (SNV), multiplicative scatter correction (MSC), and principal component analysis (PCA)] were performed on the data using the following commercial software packages: Vision (Foss NIRSystems, Silver Spring, MD), Grams (Galactic Industries Corp., Salem, NH), Spectrum Quant+, and SIMCA Analysis (Perkin Elmer Corp., Norwalk, CT). TableCurve2D^{TM} (SPSS Science, Chicago, IL) was used for end point determination.

Near-Infrared Imaging

The lids of the V-blender were removed to enable access to the top surface of the powder for imaging studies. The NIR imaging configuration is shown in Figure 2. Two heat lamps (250W, PC37771, near-infrared/infrared lamps, General Electric, Cleveland, OH) were used for uniform illumination of the sample. NIR radiation was collected with an InSb focal plane array camera (IRC 160, LN_2 cooled Cincinnati Electronics) with a focusing lens and filters (Edmund Scientific) attached to the front end. Images were collected using six bandpass filters (1678, 1944, 2098, 2180, 2230, 2312 nm) that encompassed lactose and SA peaks. The imaging system remained stationary and the blender platform was rotated to allow image collection from both sides of the blender. Black and white reference materials were incorporated into every image for scatter correction. All preprocessing image analysis was performed with Matlab 5.0 software (Mathworks, Inc., Natick, MA). In all imaging experiments, the progress of mixing was also monitored by NIR spectroscopy and the UV reference method to allow comparison of the different techniques.

Salicylic Acid Assay

To dissolve the active ingredient, weighed powder samples were mixed with methanol and then diluted to volume with water. SA concentrations were measured using a Lambda 2S UV/VIS spectrometer (Perkin Elmer Corp., Norwalk, CT) at 296.9 nm. The Calibration curve for SA (absorbance versus concentration) was linear over the range 0–40 μg/mL ($r^2 = 0.9999$). The precision of the method was evaluated by preparing the calibration on three different days (RSD $< 1.5\%$). Accuracy was calculated to be between 100 and 103% at all concentration levels used in the calibration.

RESULTS AND DISCUSSION

Ultraviolet Spectroscopy Analysis

UV spectroscopy is considered a standard method for the determination of content uniformity of powder blends. The percent potency results for the 7% SA powder blend as determined by UV are shown in Figure 3. SA was loaded into the blender from the left side causing the SA content to be initially higher on the left side of the blender compared with the right side. However, at 10 min, both sides reached approximately the same value and, by 16 min, the blend had reached an acceptable level of homogeneity. The end point determination is based on mean and standard deviation (SD) acceptance criteria stated in the PDA technical report No. 25.[16] The PDA report No. 25 calls for all samples to be between 90 and 110% of the label claim and for the RSD to be <5%. The blender was filled to 90% of its loading capacity, which explains the slow rate of mixing observed.[15]

The percent potency and percent RSD results obtained from the UV analysis for the different blends (3, 7, and 11% A and 11% B) are summarized in Table 1. End points of the different blends are marked in bold. The 11% A and the 11% B SA blends differ in that the former was weighed and used directly, whereas the latter was

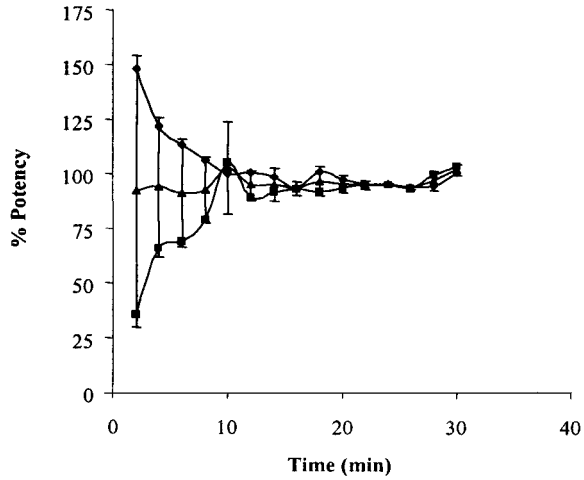

Figure 3. UV potency results ($n = 6$) for the 7% SA powder blend from the left side ($n = 3$; ◆), right side ($n = 3$; ■), and average potency (▲). Error bars indicate percent RSD.

Table 1. Results of the UV Analysis for All the Blends

	Blend							
	3%		7%		11% A		11% B	
Time[a]	% Potency	% RSD	% Potency	% RSD	% Potency	% RSD	% Potency	% RSD
2	—	—	91.99	67.49	87.52	49.70	91.60	29.61
4	—	—	93.88	34.09	114.62	53.43	99.90	25.08
5	77.73	24.50	—	—	—	—	—	—
6	—	—	91.00	27.16	89.42	21.48	95.65	10.50
8	—	—	92.54	16.46	94.71	20.94	95.97	7.73
10	84.33	12.32	102.64	20.57	90.62	12.70	**96.50**	**4.71**
12	—	—	94.88	7.28	88.81	7.09	97.57	2.03
14	—	—	97.07	7.95	**90.69**	**4.23**	95.66	2.44
15	90.14	27.63	—	—	—	—	—	—
16	—	—	**93.42**	**3.52**	91.37	4.90	94.95	4.75
18	92.02	19.91	96.79	7.22	89.70	3.17	97.91	5.42
20	—	—	95.69	4.20	115.84	33.14	95.46	0.51
21	92.81	24.82	—	—	—	—	—	—
22	—	—	95.23	2.04	93.78	2.10	100.98	4.35
24	89.79	5.44	95.42	0.84	93.52	0.84	97.92	2.98
26	—	—	93.62	0.73	94.94	1.59	96.23	0.93
27	99.40	7.52	—	—	—	—	—	—
28	—	—	97.13	4.63	98.03	7.83	96.68	0.71
30	96.73	10.08	102.13	2.46	93.22	2.56	98.64	4.64

[a]Time measured in minutes.

stored in a container for 1 week and shaken intermittently before blending. Based on established end point criteria, the 3% SA powder blend never reaches homogeneity. Although UV samples were collected every 5 min for the first 15 min, sampling frequency was not adequate to capture the true end point. It can be seen from Table 1 that there is a decrease in blend homogeneity for 7 and 11% A and 11% B powder blends after the end point is attained. This phenomenon has been reported in previous blend studies[13] and can be attributed to particle attrition, change in particle size distribution, build-up of static charge, etc. This result indicates the importance of exactly identifying the time at which the end point is achieved to avoid subsequent loss of homogeneity on mixing for unnecessarily longer times.

Near-Infrared Spectroscopy

NIR can be implemented as an on-line monitoring tool, providing sufficient sampling frequency to give real-time control of the blending process. NIR spectra of the individual constituents, SA and lactose, are shown in Figure 4. Spectral features of the two components are quite distinct and can easily be used to monitor the blending process. As the blend reaches homogeneity, NIR spectra of the blend reach an equilibrium intensity level, as seen in Figure 5. The 1656 nm 2nd derivative band, evident as a trough, is a strong indicator of SA, the active ingredient. Four spectra (t_{24}–t_{30}) from a homogeneous blend are displayed as overlapping traces. The spectra displayed were collected from window 1. The lack of a band at $t = 0$ is due to the absence of SA in front of that window prior to blending.

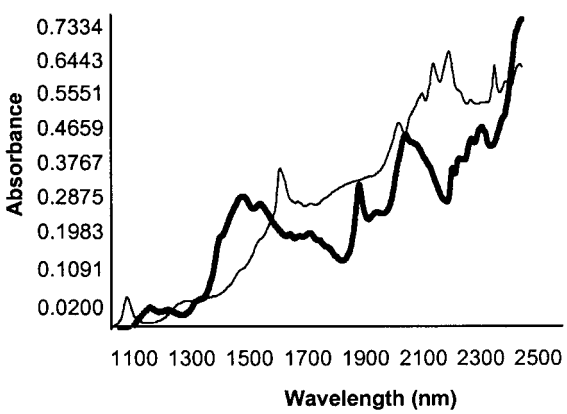

Figure 4. NIR spectra of lactose (▬) and SA (—).

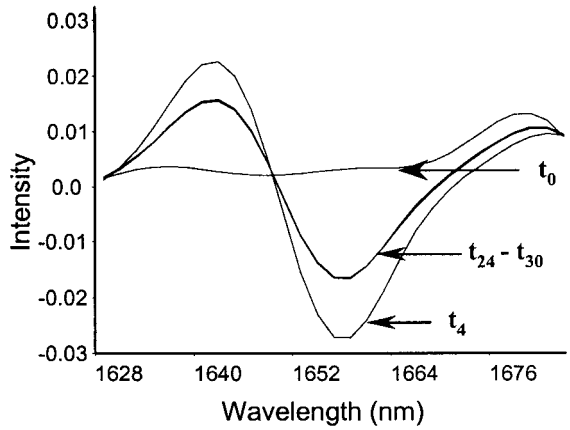

Figure 5. IR 2nd derivative spectra of 7% SA powder blend focusing on the SA peak at 1656 nm. The absorbance peak appears as a trough in the 2nd derivative spectrum.

End Point Determination by Qualitative Pattern Recognition Methods

Pattern recognition methods have been recognized as a valuable and very sensitive tool for evaluation of NIR spectra arising from homogeneity studies.[12,13,17,18] A principal component plot of the 7% SA blending experiment is shown in Figure 6. Such plots, where each point represents a single spectrum, are valuable for visual analysis of the data. Various algorithms for pattern recognition or cluster analysis are then applied to provide statistical evidence regarding the discrimination of spectra. In this case, SIMCA[19] was used to provide 98% recognition rates for identification of the NIR spectra arising from a homogeneous blend (spectra from $t = 16$–30 min). The path of the spectra as the blend progresses is illustrated in Figure 6. "A" represents spectra collected at $t = 0$ from five of the six windows that were displaced away from that of the sixth window at the same time point (as depicted by the arrow) because the latter had primarily SA in front of it before mixing started. "B" and "C" represent spectra collected from the windows on the right and the left arm of the blender, respectively, prior to achievement of homogeneity. Spectra from the left arm (windows 1, 2, and 3) show less scatter compared with their counterparts from the right arm (windows 4, 5, and 6). The variability trend observed with the NIR spectra agrees with that seen in the UV data and listed in Table 2. This result can be attributed to loading the powder into the blender from the left side, which led to slow migration of SA across

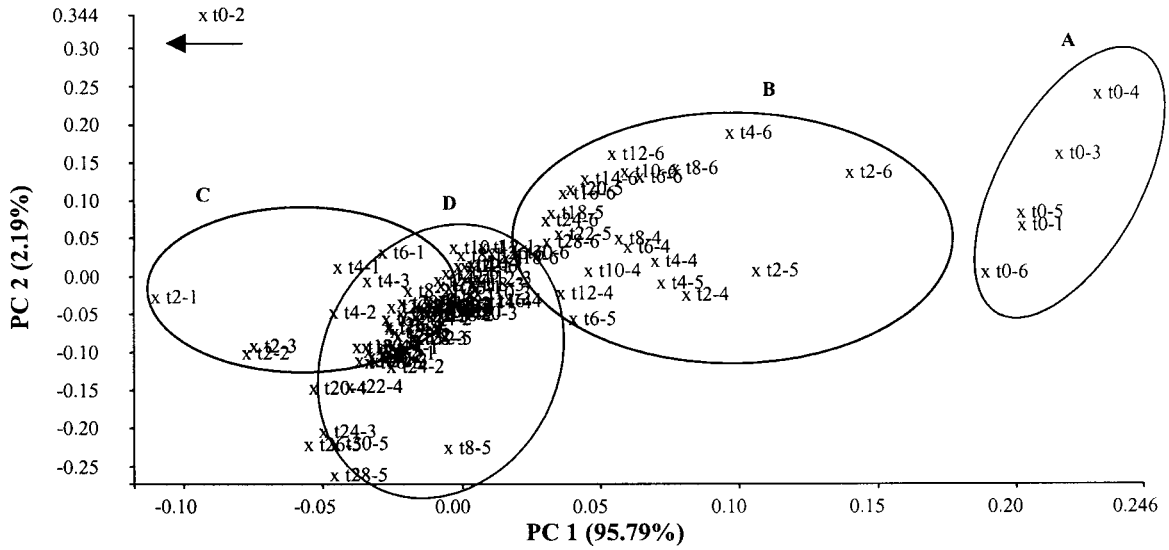

Figure 6. Cluster analysis of the 7% SA powder blend showing the spectra as points projected in multidimensional space and each labeled as *t*n-w (*t*n: time in minutes; w: window number): A ($t = 0$); B (premixing, right side of the blender), C (premixing, left side of the blender), D (homogeneous blend). The arrow points toward the direction where *t*0-2 is located.

the vertical plane of symmetry as commonly observed in mixing studies involving the V-blender.[15] As blending approaches homogeneity, spectra from both arms converge forming cluster "D". Based on the UV reference results, spectra from "D" represent a well-mixed blend. Spectra from homogeneous samples, like those from "D", can be utilized as a training set of known, well-mixed samples against which other, unknown samples (spectra from future blends) can be tested for homogeneity. An added advantage of this approach is that potency is tested simultaneously with spectral variability.

End Point Determination by Curve Fitting to Standard Deviation Data

Sekulic et al. have described a moving block SD calculation for determination of the end point of mixing.[20] In their method, data are arranged into a time by wavelength matrix. A new matrix is calculated over all wavelengths by determining the SD of intensity values for the numerous time blocks. Finally, a mean value is calculated from each of the resulting SD spectra over all wavelengths. The mean SD can be plotted as a function of time. The blending end point is determined to be the time point at which the mean SD profile reaches a minimum value.

In our study, SD was calculated from pooled variance in a moving window of three time points for the end point calculations from individual windows. Eighteen points (three time points by six windows) were utilized for calculations involving all windows. Rather than using the entire

Table 2. Calculated % RSD Values for the 7% SA Powder Blend from the Right and Left Arms of the Blender

	% RSD	
Time[a]	Left	Right
2	4.94	15.44
4	0.90	20.14
6	4.17	0.67
8	1.76	3.60
10	1.88	31.50
12	4.58	1.65
14	7.62	7.58
16	3.05	4.63
18	7.70	0.77
20	2.92	4.95
22	2.95	1.21
24	1.07	0.37
26	0.12	1.00
28	2.06	5.30
30	1.56	2.69

[a]Time measured in minutes.

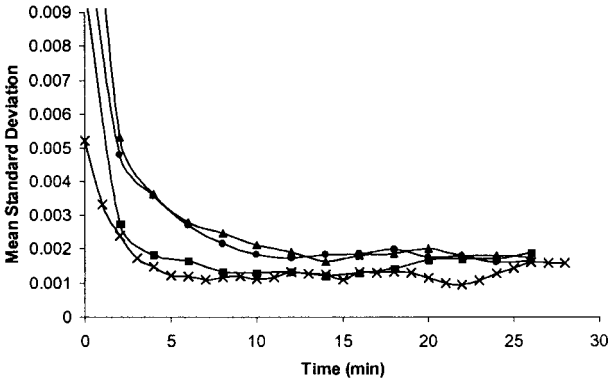

Figure 7. Mean SD profiles of 3% (×), 7% (▲), 11% A (●), and 11% B (■) SA powder blends as a function of time using all windows.

spectrum, PCA was used to select the wavelengths (1130, 1656, 1934, 2070, 2092, 2138, and 2188 nm) corresponding to SA and lactose absorbance bands to be used for the calculation. This method improved the accuracy of end point determination by eliminating regions of the spectra that did not correlate strongly with active/excipient concentrations. The first derivative of the mean SD profile was calculated. The point at which the resultant derivative curve crosses zero was taken as the end point of mixing.

Concentration Effects

Plots of mean SD versus time (using all windows) for the various blends of SA (3, 7, and 11%) are shown in Figure 7. The mean standard deviation decreases as a function of time, indicating that the blends are approaching homogeneity. Each concentration provides a different standard deviation/time profile, demonstrating that component concentration has a significant effect on the mixing process. Moreover, the two 11% blends with identical composition provided very different SD–time profiles. This difference is due to the different environmental conditions in which the two blends were run: 11% A was blended immediately after weighing components, whereas 11% B was held in a container for 1 week before blending. Such data indicate the importance of monitoring each individual blend. Numerous factors can cause variability in the mixing end point, even for blends of identical composition. NIR can prove useful in this respect because it minimizes the time required for analyzing the samples relative to traditional analytical methods.

Multiple Sampling and Spatial Variation Effects

NIR sampling ports were installed at six different positions around the blender to determine how spatial positioning and the number of sampling points influence end point calculation. Sampling locations were chosen to cover the full range of spatial possibilities on the V-blender from high to low, left to right, and front to back.

An SD calculation was used to determine the end point of mixing for each individual window in the 7, 11% A and 11% B SA blends. Results are listed in Table 3. Three different preprocessing treatments including 2nd derivative, SNV, and MSC, were applied to the spectral data for removal of linear baseline shifting. It is evident from Table 3 that one sampling point is inadequate for end point determination. Not only do the end points vary for individual windows, but there are also inconsistencies across the three different pretreatments. These results are in agreement

Table 3. End-point Determination for Individual Windows of the 7%, 11% A, and 11% B SA Powder Blends[a]

Blend	Spectral pretreatment	End point (min)						Reference End Point
		1	2	3	4	5	6	
7%	2nd Derivative	9.59	8.67	18.06	4.37	15.84	15.25	14.92
	SNV	10.24	22.75	10.93	3.91	9.48	8.43	
	MSC	10.22	21.63	10.95	3.89	9.47	8.44	
11% A	2nd Derivative	7.52	9.41	13.37	3.25	21.36	5.09	13.27
	SNV	8.65	8.43	15.75	3.04	20.60	6.36	
	MSC	7.80	8.42	15.74	3.05	20.67	6.37	
11% B	2nd Derivative	5.54	5.80	6.43	8.58		20.49	9.21
	SNV	21.86	6.48	6.30	7.60	—[b]	4.74	
	MSC	21.92	6.46	6.27	8.58		4.69	

[a]Wavelengths used: 1130, 1656, 1934, 2070, 2092, 2138, and 2188 nm.
[b]Date not available.

Table 4. End-Point Determination for all Blends using All Windows[a]

	End Point (min)			
Blend	2nd Derivative	SNV	MSC	Reference
3%	7.21	7.49	7.48	—
7%	15.35	14.34	14.86	14.92
11% A	13.80	12.72	12.73	13.27
11% B	9.51	10.10	10.10	9.21

[a]Wavelengths used: 1130, 1656, 1934, 2070, 2092, 2138, 2188.

with the powder blend studies performed by Muzzio et al., in which the key parameter controlling the accuracy of blend analysis was the number of samples analyzed.[21] Using data from all six optical ports improves the accuracy of end point estimation, as seen in Table 4. The end point results for the 7%, 11% A, and 11% B SA powder blends from NIR spectral data correlate well with the reference UV analytical method. Because of the high correlation between UV and NIR methods for all other blends, we assume that the results for the 3% SA blend end point occurring at ~7 min are accurate.

Near-Infrared Imaging

NIR spectroscopy results indicate the necessity of using multiple sampling points for mixing end point determination. Based on this same principle, NIR imaging experiments provide measurements from a large mass of sample. The larger sample mass could be valuable in improving the statistical confidence of the end point determination and insuring a more accurate measure of blend homogeneity. To take advantage of such improved statistical confidence, estimates of the sample mass would be required.

NIR images were collected using discrete bandpass filters encompassing absorption bands of SA and lactose. Before data analysis, the images were background corrected and converted to log $(1/R)$ scale, which is linear with respect to concentration. A multiplicative scatter correction was applied to each image using the black and white reference spectra for determination of an ideal or average spectrum.

Approximately two thirds of the entire top surface of the powder within one side of the blender was imaged, as seen in Figures 8A–E.

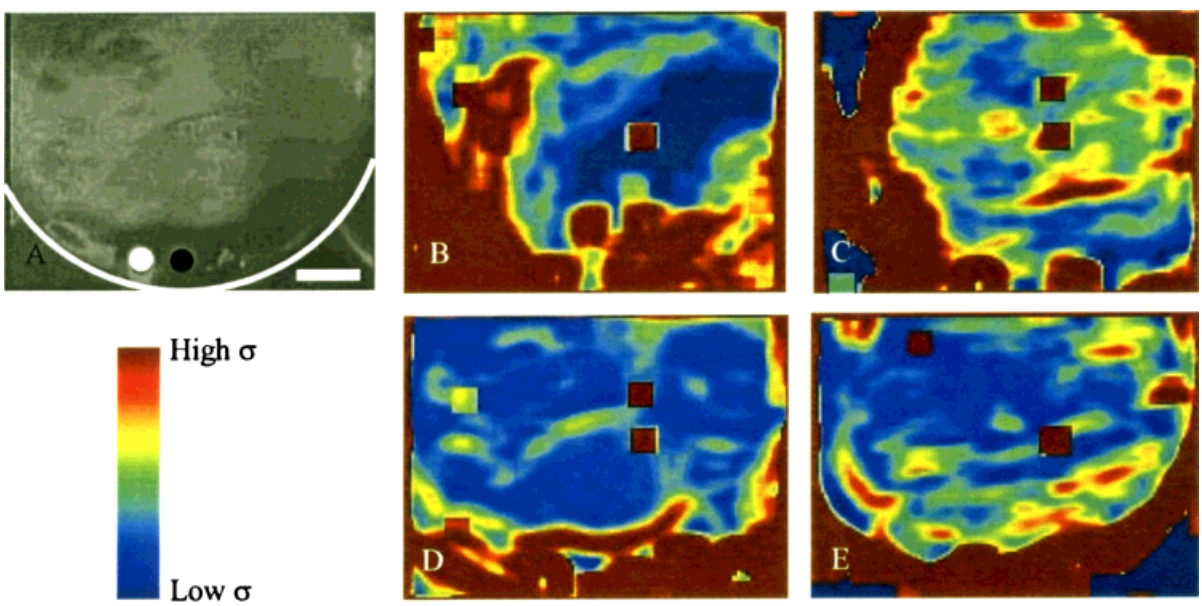

Figure 8. Moving block SD images of 7% SA powder blend: (A) white light image; (B) $t = 0$ min; (C) $t = 6$ min; (D) $t = 14$ min; (E) $t = 30$ min. The images were collected at the SA absorbance band of 1656 nm and the size bar in (A) corresponds to 2.5 cm.

The blender was rotated for 30 min, with sample collection at 2-min intervals. Figure 8A is a white light image of the surface of the blender taken without the filters in place and it shows the edge of the blender and the location of the round reference materials. The SD calculation was performed on images 8B–E for the 7% SA blend by applying a moving block window (10 × 10 pixels in size) to each image collected with the 1678-nm filter. The image collected at 1678 nm encompasses the diffuse reflectance signal of the SA (the active ingredient). The calculated SD provides an estimate of variability and approaches a minimum when the mixing end point is reached. The images in Figure 8B–E are slightly shifted relative to each other because of the rotation of the entire blender at each time point to capture images from the left and right sides.

Image color has been scaled according to the minimum and maximum SD values calculated at each pixel inside the blender, where a high SD value corresponds to red and a low SD value corresponds to blue. At time 0 min (Figure 8B), a relatively low SD is observed across the entire image. This result is attributed to SA being loaded on the top surface of the powder bed and providing a low SD due to the image capturing a view of a single component rather than being due to the appearance of a homogeneous blend. As the blend progresses, the variability first increases, as seen in Figure 8C ($t = 6$ min), drops to a minimum in Figure 8D ($t = 14$ min), and then begins to increase again in Figure 8E ($t = 30$ min). A single SD value calculated over all image pixels at each time point is shown in Figure 9.

Based on Figures 8 and 9, homogeneity is reached between 14 and 16 min. The powder begins to "de-mix" or segregate as mixing continues beyond the time when homogeneity was reached, exhibiting increased variability beyond 20 min. This phenomenon is attributed to particle size and size distribution changes arising from attrition due to continued blending and has been seen in other studies performed by this lab.[13] NIR imaging data correlates well with the UV reference data, as shown in Figure 3. Both the NIR imaging and UV reference method display a large standard deviation at 10 min, a minimum at 14–16 min, and a spike at 18 min. Further comparison between the NIR imaging and traditional NIR reflectance measurements for the 7% SA powder blend indicates that the end points calculated by the two methods occur at roughly the same time point (14–16 min). Although the more traditional NIR measurements allowed blend sampling at different depths in the powder bed, the volume of powder captured by the imaging technique is significantly larger. Coupling both techniques might provide an even more robust tool for monitoring powder blending.

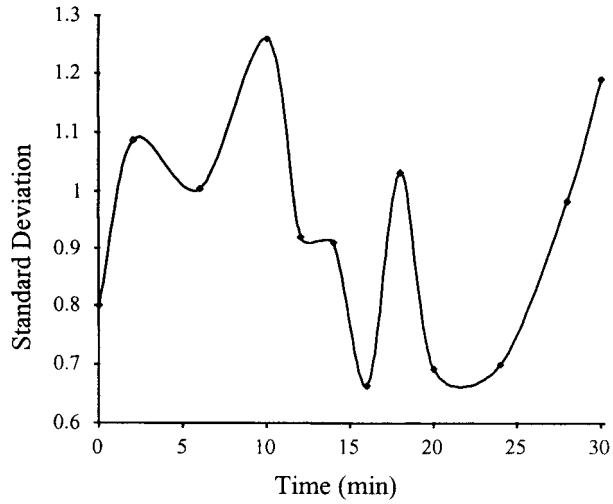

Figure 9. SD of all image pixels as a function of time.

CONCLUSIONS

Powder blending was monitored by NIR spectroscopy and imaging with UV spectroscopy used as the reference method. A variety of qualitative and quantitative algorithms are valuable for determination of powder blend homogeneity. It was evident that environmental conditions and component concentration had an impact on the blending process. Consequently, monitoring every blend could provide an advantage in terms of improved product quality. To insure accurate measurement of the blend homogeneity, multiple sampling points were essential. Studies are underway in our lab to determine the necessary number and optimum spatial distribution of the optical windows on the blender. The results obtained from NIR spectroscopy and imaging experiments agreed well with the UV reference analysis method. However, as a rapid and noninvasive technique, NIR methods reduce sampling errors and provide the possibility of on-line end point determination, leading to a potentially significant improvement over conventional analytical methods.

ACKNOWLEDGMENTS

Perkin Elmer Corp., Salem, NH and Foss NIR-Systems, Silver Spring, MD are acknowledged for the NIR instrumentation and accessories used in this work.

REFERENCES

1. Berman J, Schoeneman A, Shelton JT. 1996. Unit dose sampling: A tale of two thieves. Drug Dev Ind Pharm 22(11):1121–1132.
2. Berman J, Planchard JA. 1995. Blend uniformity and unit dose sampling. Drug Dev Ind Pharm 21(11):1257–1283.
3. Guentensberger J, Lameiro P, Nyhuis A, O'Connell B, Tigner S. 1996. A statistical approach to blend uniformity acceptance criteria. Drug Dev Ind Pharm 22(11):1055–1061.
4. Chang R, Shukla J, Buehler J. 1996. An evaluation of a unit-dose compacting sample thief and a discussion of content uniformity testing and blending validation issues. Drug Dev Ind Pharm 22(9&10):1031–1035.
5. Muzzio FJ, Roddy M, Brone D, Alexander AW, Sudah O. 1999. An improved powder-sampling tool. Pharm Technol 23(4):92–110.
6. Plugge W, Van der Vlies C. 1993. Near-infrared spectroscopy as an alternative to assess compliance of ampicillin trihydrate with compendial specifications. J Pharm Biomed Anal 11:435–442.
7. Corti P, Dreassi E, Ceramelli G, Lonardi S, Viviani R, Gravina S. 1991. Near-infrared reflectance spectroscopy applied to pharmaceutical quality control. Identification and assay of cephalosporins. Analysis 19:198–204.
8. Drennen JK, Lodder RA. 1990. Nondestructive near-infrared analysis of intact tablets for determination of degradation products. J Pharm Sci 79(7):622–627.
9. Kirsch JD, Drennen JK. 1995. Determination of film-coated tablet parameters by near-infrared spectroscopy. J Pharm Biomed Anal 13:1273–1281.
10. Kirsch JD, Drennen JK. 1999. Nondestructive tablet hardness testing by near-infrared spectroscopy: A new and robust spectral best-fit algorithm. J Pharm Biomed Anal 19:351–362.
11. Galante L, Brinkley M, Drennen J, Lodder R. 1990. Near-infrared spectrometry of microorganisms in liquid pharmaceuticals. Anal Chem 62:2514–2521.
12. Drennen JK, Lodder RA. 1993. Pharmaceutical applications of near-infrared spectrometry. Adv Near-Infrared Meas 1:93–112.
13. Wargo D, Drennen JK. 1996. Near-infrared spectroscopic characterization of pharmaceutical powder blends. J Pharm Biomed Anal 14:1415–1423.
14. Sekulic SS, Ward II HW, Brannegan DR, Stanley ED, Evans CL, Sciavolino ST, Hailey PA, Aldridge PK. 1996. On-line monitoring of powder blend homogeneity by near-infrared spectroscopy. Anal Chem 68:509–513.
15. Brone D, Alexander A, Muzzio FJ. 1998. Quantitative characterization of mixing of dry powders in V-blenders. AIChE J 44(2):271–278.
16. Berman J, Elinsiki DE, Gonzales CR, Hofer JD, Jimenez PJ, Planchard JA, Tlachac RJ, Vogel PF. 1997. Blend uniformity analysis: Validation and in-process testing. Technical Report No. 25. PDA 51:S1–S99.
17. Drennen JK. 1990. A "noise" in pharmaceutical analysis: Near-infrared outside/inside space evaluation. Ph.D. Thesis, University of Kentucky, pp 248–296.
18. Cuesta Sánchez F, Toft J, Van Den Bogaert B, Massart DL, Dive SS, Hailey P. 1995. Monitoring power blanding by NIR spectroscopy. Fresnius J Anal Chem 352:771–778.
19. Lavine BK. 1992. Signal processing and data analysis. In: Haswell SJ, editor. Practical guide to chemometrics. New York: Marcel Dekker, Inc. pp. 225–227.
20. Sekulic SS, Wakeman J, Doherty P, Hailey PA. 1998. Automated system for the on-line monitoring of powder blending processes using near-infrared spectroscopy Part II. Qualitative approaches to blend evaluation. J Pharm Biomed Anal 17:1285–1309.
21. Muzzio FJ, Robinson P, Wightman C, Brone D. 1997. Sampling practices in powder blending. Int J Pharm 155:153–178.